Dual Band Compact Square Microstrip Antenna for GSM and GPS Applications

Aarti G. Ambekar[*] **and Amit A. Deshmukh**

Abstract—The design of a half U-slot loaded square microstrip antenna is proposed for the dual band response offering circular polarization in the second band. On a substrate with thickness of $0.06\lambda_g$, the half U-slot tunes the spacing in between TM_{10}, TM_{01}, and TM_{11} resonant modes of the square patch to achieve dual band characteristics. In the two bands, measured impedance bandwidths of 6.49% and 17.36% with a broadside gain $> 7.0\,\text{dBi}$ are achieved. Against the equivalent square patch, the proposed dual band antenna offers 8% reduction in the patch area. With the achieved antenna characteristics, the proposed configurations satisfy the requirements of GSM 750/GPS L5 band applications.

1. INTRODUCTION

Modern day wireless communication systems prefer antennas with a small profile, providing diversity or agility in terms of frequency and polarization that avoids the losses due to the multi-path propagation and channel bandwidth [1, 2, 4]. To satisfy these requirements, multiband antennas with dual polarizations are frequently used. Due to the small profile, microstrip antenna (MSA) is widely used in applications for realizing the multiband response offering dual polarizations [1, 3]. The realization of dual polarized multiband response in MSA is the result of various methods like slots or stubs, use of stack resonators, and different feeding techniques, as per the reported literature [5–8]. A dual band circular polarized (CP) configuration is reported in [9] that operates in 2100 & 3600 MHz frequency spectrum. This reported work lacks in providing an in-depth explanation for the effects of the eccentric ring patches and arc shape feed, for realizing the dual band response. In addition, the theoretical approach for deriving the empirical formulation proposed, based on the antenna parameters is missing. The impedance and axial ratio (AR) bandwidth are small for the compact dual band stacked CP MSAs reported in [10–12], though they are fabricated on a thicker substrate. A design of single feed dual band and dual polarized antenna is reported in [13] for the GPS application. It yields impedance bandwidth of 1.5 and 2% in each band. In this design, multiple slots are embedded on the main patch, which increases the design complexity. A dual band CP MSA for a small frequency ratio using slots and stubs is reported in [14]. A multiband CP antenna for 5G/B5G applications using multiple patches embedded with slots is reported in [15]. Here, the antenna size increases due to the multiple patches. A slotted patch antenna for CP response using shorting posts for GNSS application is reported in [16]. Due to the presence of short and slot together, the design optimization is complex. Using the combination of slots and stubs, a triple band CP antenna is reported in [17]. The use of reconfigurable techniques in multiband dual polarized antennas increases the fabrication complexity [18–20]. Various multiband designs of U-slot cut patch antenna as reported in [26] do not provide a small frequency ratio and agility. Thus, in most of the reported work, a simple configuration to provide dual band response with small frequency ratio and polarization agility, with appreciable values of gain and bandwidth is missing. Also, a design methodology to realize a similar configuration as per the desired frequency band is not given.

In this paper, at first an offset coaxial feed square MSA (SMSA) is discussed on an air suspended FR4 substrate ($\varepsilon_r = 4.3$, $h = 0.16$ cm), with a total substrate thickness of $0.06\lambda_g$ in 850 MHz frequency band. An N-type connector is used to feed the MSA. The resonant modes of basic SMSA are analyzed. At the fundamental mode, it yields bandwidth of 100 MHz (10%). However, for the possible dual band dual polarized response, an impedance matching at higher order orthogonal modes is not observed. To discover the possibility of dual band dual polarized (DP) or circularly polarized (CP) response, an asymmetrical offset half U-slot is embedded at the bottom edge of the square patch. The half U-slot optimizes the inter spacing in between the fundamental TM_{10} and TM_{01} modes as well as their spacing with respect to TM_{11} mode that yields dual band response with dual and circular polarizations in the second band. An optimum response covering the two frequency bands: 745 to 795 MHz and 1005 to 1196 MHz, thus realizing measured impedance bandwidth of 6.49 and 17.36% with a broadside gain > 7.0 dBi, is obtained. In addition, the slot cut SMSA shows CP response in the second band with the measured AR bandwidth of 36 MHz (3.1%). By studying the modal current distributions, resonant length formulations at the modified TM_{10}, TM_{01}, and TM_{11} resonant modes are proposed. Using them, a design methodology to realize a similar dual band SMSA in different frequency bands is presented, which shows similar dual band response. Based on the results obtained, the proposed compact design is suitable for the GSM 750 (747.2 to 792.2 MHz) and GPS L5 band (1176.45 MHz) applications. Thus, the technical novelty in the present work lies in providing an in-depth explanation for the dual band response by analyzing the higher order modes of the compact SMSA, to offer wider impedance BW along with polarization agility. In terms of the center frequency of the first band in dual band SMSA, the proposed design offers 8% reduction in the patch area, in comparison to the equivalent SMSA without the slot. In addition, a smaller frequency ratio between the two bands is obtained. Thus, a single patch geometry modified with the slot makes the proposed design very simple in implementation as compared with the reported dual band MSAs. A detailed comparison against the reported work is given further in the paper. The proposed configuration is first simulated using CST Microwave Studio [22]. In the simulation and measurement, a square ground plane of a side length of 30 cm is used. High-frequency instruments namely ZVH-8, FSC 6, and SMB-100A are used for experimental validation. The radiation pattern and gain measurements are carried out using reference wideband horn antennas. Three antenna method is used in the gain measurement.

2. DUAL BAND HALF U-SLOT LOADED COMPACT SMSA

U-slot or half U-slot cut MSAs are design friendly configurations and when being realized on thicker or thinner substrate, yield wideband [21] or multi-band [23] response, offering polarization purity in the radiation pattern. In terms of the slot geometry, U-slot is a symmetrical structure as against the half U-slot [21]. In addition, the design with half U-slot offers 50% patch size reduction [21]. The CP designs of U-slot employing a square patch have been reported in the literature [28–32]. Hence, an asymmetry in the half U-slot design can be exploited to yield polarization agile or CP configurations. But in the reported work, compact designs of half U-slot cut configurations have not been reported for dual band dual or circularly polarized response, which are needed in frequency and polarization agile systems. A compact wideband design of a half U-slot cut rectangular MSA fabricated on an air suspended FR4 substrate with a total thickness of $0.065\lambda_g$ yields BW of 130 MHz (14.6%), around the fundamental TM_{10} mode, in 900 MHz frequency band [21]. In that design, although $L > W$ and an offset feed and half U-slot was employed, an excitation of the orthogonal mode for the possible polarization agile wide or multi-band response is not observed. This is attributed to the symmetrical half U-slot and the use of a rectangular patch in the wideband design. To realize an orthogonal polarization over the wide or multi-band response, orthogonal surface currents on the patch are needed. To realize this, a square patch ($L = W$) is considered in the present design that is fabricated on similar FR4 substrate parameters, as air gap 'h_a' = 2.0 cm. The basic SMSA dimensions are selected as $L = W = 12$ cm, $L_{sub} = 16$ cm, which are less than the dimensions reported in [21]. This is for satisfying the requirements of GPS L5 band. An offset coaxial feed is placed on the patch edge as shown in Figs. 1(a) and (b). For the identification of the basic SMSA modes, the patch is simulated for 'x_f, y_f' = 1.6, 1.0 cm, and the resonant curve plot and current distributions at the observed resonant peaks are shown in Figs. 1(c)–(e).

The '+' and '−' signs in the current plots indicate the field polarity. At the first peak, due
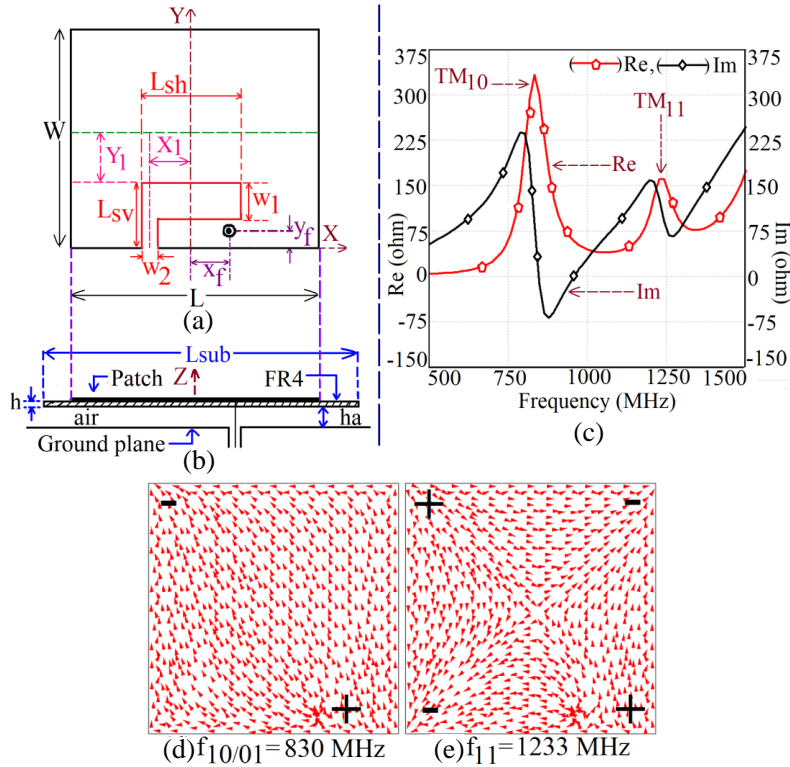
Figure 1. (a) Top and (b) side views of co-axially fed SMSA loaded with half U-slot, (c) resonance curve plot and (d), (e) surface current distributions at observed resonant modes, for SMSA.

to the square patch, currents exhibit one half wavelength variation along the diagonal length. This is due to the close proximity of TM_{10} and TM_{01} modes. At the second peak, one half wavelength variation along the patch length and width is observed corresponding to TM_{11} mode. These modal identifications for the SMSA are well documented in the reported literature and hence not discussed here in more details [1, 2]. For realizing the dual band dual polarized response, appropriate spacing between the TM_{10} and TM_{01} modes is needed along with the impedance matching at TM_{11} mode. Also modifications in the surface current vectors at TM_{11} mode are needed to yield the broadside pattern. To realize all these, the technique of slot or stub can be used. In present work, slot cut technique is selected as it offers compactness along with the frequency tuning in between the resonant modes and modifications in current vector directions. Thus, the configuration of half U-slot cut SMSA is shown in Fig. 1(a). An offset slot is selected since it will help in tuning of either TM_{10} or TM_{01} modes with respect to other modes as well as it will not realize uni-directional current variation over the patch [24, 27]. This will assist in orthogonal current components to realize the dual polarizations. Further to assist the same functionality, an unequal slot width in the two arms of the half U-slot is selected. For optimizing the configuration, a detailed parametric study is carried out for the half U-slot dimensions, i.e., vertical length 'L_{sv}' and horizontal length 'L_{sh}', for $w_1 = 1.0$ and $w_2 = 2.4$ cm.

The resonance curve plots for half U-slot length variations are shown in Figs. 2(a)–(c) which explain the effects of the slot dimension on the frequency and input impedance at the patch resonant modes. With an increase of 'L_{sv}', TM_{10} and TM_{11} mode frequencies decrease, as their current distribution is orthogonal to the slot length. Since the vertical slot length 'L_{sv}' is not present in the patch center, the reduction in TM_{10} mode frequency is smaller. For $L_{sv} = 4.0$ cm, a horizontal separation between TM_{01} and TM_{10} modes takes place, and two resonant peaks are observed, as shown in Fig. 2(a). To retain the compactness of half U-slot, $L_{sv} = 4.0$ cm is kept constant. For further tuning of the response for realizing the dual band characteristics, 'L_{sh}' is increased further, as shown in Figs. 2(b) and (c). With further increase in 'L_{sh}', TM_{10} and TM_{11} mode frequencies are reduced whereas the TM_{01} mode frequency remains constant. Thus, the half U-slot yields frequency tuning in between these three resonant modes.
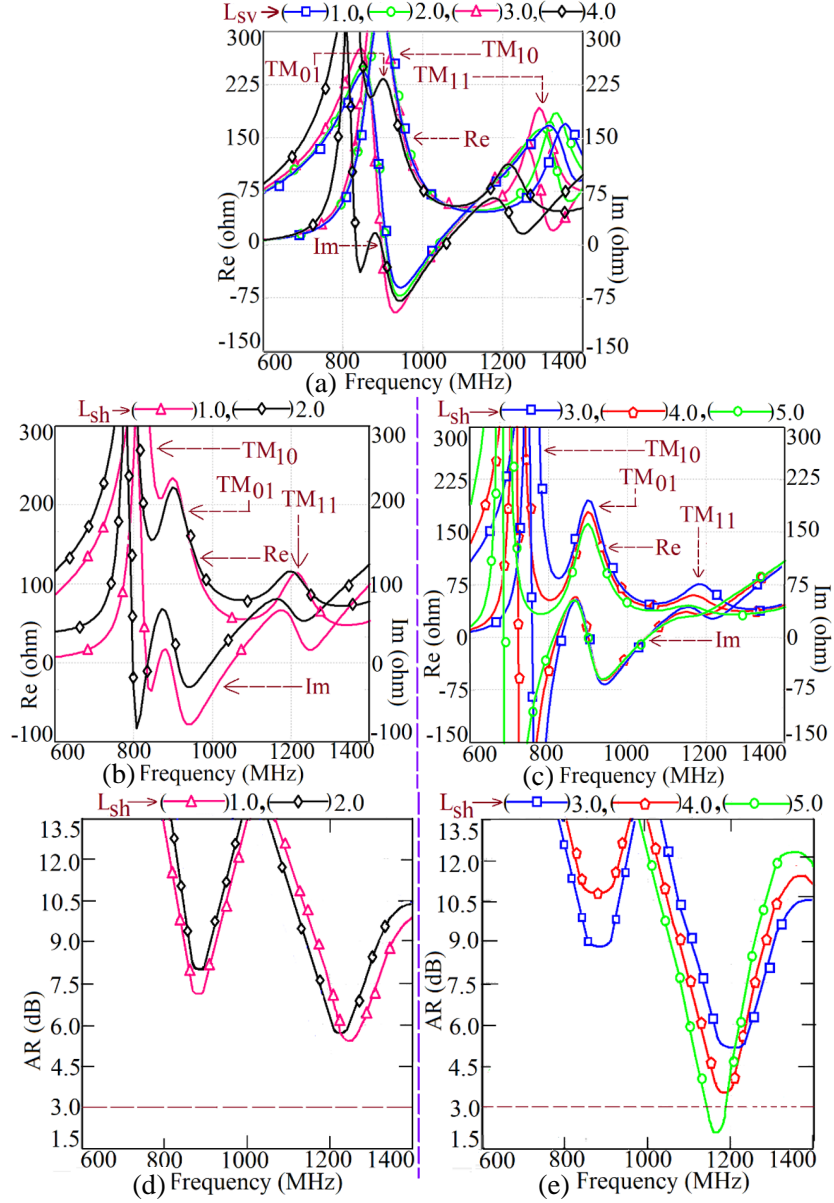
Figure 2. Resonance curve plots for variations in (a) vertical slot length 'L_{sv}', and (b), (c) horizontal slot length 'L_{sh}' and (d), (e) AR bandwidth plots against slot length variation for half U-slot cut SMSA.

As observed from the resonance curve plots, the input impedance at TM_{01} and TM_{11} modes is reduced, but the impedance at modified TM_{10} mode increases. With an increase in the horizontal half U-slot length, the AR value around the modified TM_{11} mode frequency decreases, leading to the possible CP response as shown in Figs. 2(d), (e). However, due to the separation between TM_{10} and TM_{01} resonant modes, AR value increases in the lower frequency band, i.e., nearer to modified TM_{01} mode frequency. The surface current distribution at three resonant modes for $L_{sh} = 5.0$ cm is shown in Figs. 3(a)–(c). At the modified TM_{10} mode, currents vary along the patch length, but this mode does not yield operational frequency band for VSWR < 2, since the input impedance is very high. At TM_{01} mode, current contribution is along the patch width with input impedance below $100\,\Omega$, thereby realizing first of the dual band response. At TM_{11} mode, contribution of the surface currents along the patch length and width is present that yields CP response in the second band of the dual band response.

Thus, the proposed half U-slot cut SMSA yields optimized dual band response due to the optimum

(a)f_{10} = 604 MHz   (b)f_{01} = 833 MHz   (c)f_{11} = 1146 MHz
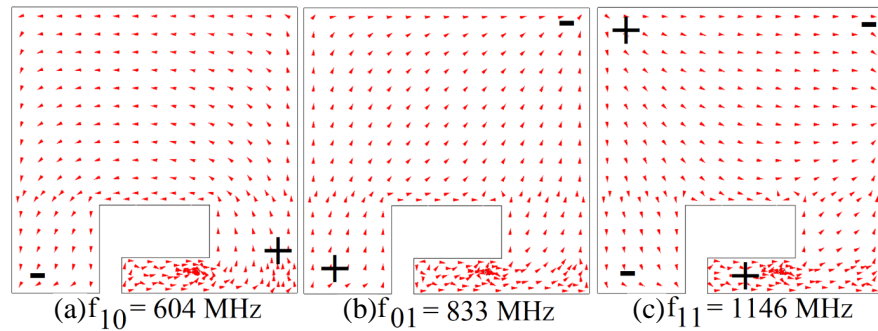
Figure 3. (a)–(c) Surface current distributions for 'L_{sh}' = 5.0 cm and 'L_{sv}' = 4.0 cm for half U-slot cut SMSA.

separation between TM_{10}, TM_{01}, and TM_{11} modes, with a CP response in the second band. As can be seen from Fig. 4(a), the selection of unequal slot width ($w_1 \neq w_2$) helps in input impedance optimization at TM_{11} mode, inside VSWR = 2 circle, which yields optimum AR bandwidth as well. The results for the optimum design for 'L_{sh}' = 5.0 cm are as shown in Fig. 4(b). The reflection coefficient (S_{11}) value is < -10 dB for the desired range of frequencies in the two bands. The simulated center frequencies in the two bands are 791 and 1113 MHz with their respective impedance bandwidths of 52 MHz (6.5%) and 187 MHz (17%). The corresponding measured values are 770 and 1100 MHz with bandwidths of 50 MHz (6.49%) and 191 MHz (17.36%), respectively.

Across the second band, the simulated AR bandwidth is 39 MHz (3.31%), while the measured value is 36 MHz (3.1%). Simulated peak broadside gains observed in the two bands are 7.5 and 7.8 dBi, while the corresponding measured values are 7.2 and 7.6 dBi. The radiation patterns observed at the center frequency of the first band and center frequency of the CP band with the respective simulated polarization field plots are shown in Figs. 4(c)–(g). The broadside radiation patterns are observed across the center frequencies of the respective bands. Since the modified TM_{01} mode is present in the first band, the E-plane is directed along $\Phi = 90°$. A higher cross polarization level (less than 6–8 dB) is observed in the first band, which is attributed to the horizontal current components due to the presence of half U-slot. At the center frequency of the AR bandwidth, the cross-polarization level in the radiation pattern is within 3 dB with respect to the corresponding co-polar level. Further at the same frequency, simulated surface current variation over the time on the half U-slot cut patch is shown in Figs. 5(a)–(d). The current vectors rotate in an anticlockwise direction, which indicates the presence of right hand CP (RHCP) response. This is also confirmed from the simulated polarization plot as shown in Fig. 4(g), where the right-hand field components are dominant. To validate the RHCP response in the measurement, a reference RHCP and left hand CP (LHCP) transmitter SMSA was designed. For the LHCP and RHCP feed excitation of SMSA, when the senses of rotations of the transmitter and receiver (half U-slot cut patch) match, the received power is maximum. For the other rotation, received power is reduced by more than 8 dB. This procedure validates the RHCP wave. The measurement setup for the same is shown in Fig. 5(e). The fabricated antenna is shown in Fig. 5(f). At the frequencies lower than the CP band, antenna shows E-plane along $\Phi = 90°$, whereas at the frequencies above the CP band, E-plane is along $\Phi = 0°$. Thus, the proposed antenna satisfies the requirements of GSM 750 (747.2 to 792.2 MHz) with respect to the first band while the second band for CP range satisfies the requirements of the GPS L5 band (1176.45 MHz, bandwidth: -12.5 to 24 MHz) with an RHCP response.

3. RESONANT LENGTH FORMULATION FOR HALF U-SLOT CUT SQUARE MSA

In the proposed half U-slot cut SMSA, the dual band response with a circular polarization in the second band is obtained due to the optimum spacing in between the TM_{10}, TM_{01}, and TM_{11} resonant modes. Thus based on the parametric study carried out for the half U-slot dimensions and the observed surface current distribution at the resonant modes, a formulation for the modified TM_{10}, TM_{01}, and TM_{11} mode resonant lengths is presented here. A variation in TM_{10} mode current vectors takes place along
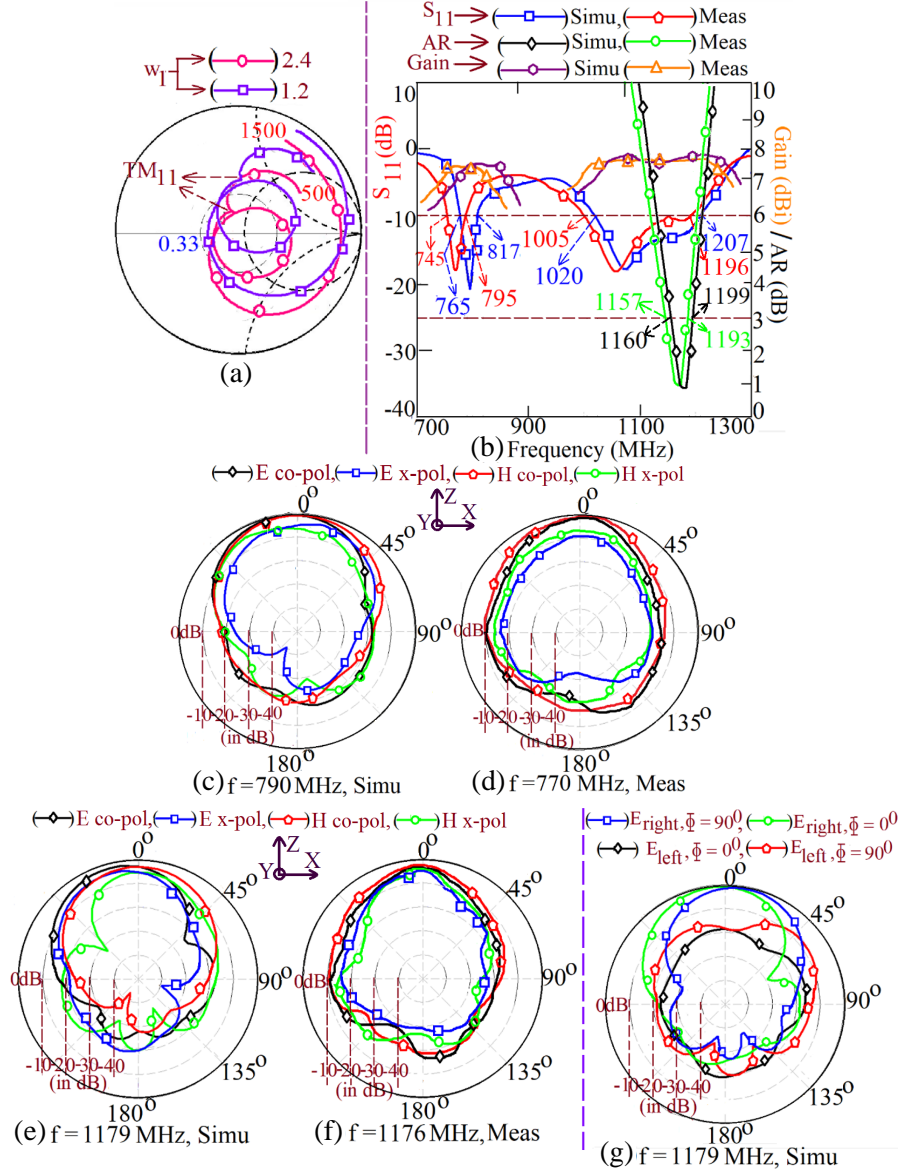
Figure 4. (a) Smith chart for 'w_1' variations, (b) S_{11}, gain and AR bandwidth plots and (c), (d) radiation patterns at the center frequency of first operating band and (e)–(g) at the center frequency of CP band, for the half U-slot cut SMSA.

the patch length, and its frequency gets affected due to the horizontal and vertical half U-slot lengths. These perturbation effects are added in the TM_{10} mode resonant length as given in Equation (1). The current components at TM_{01} mode vary along the patch width. From the parametric study it is observed that TM_{01} mode currents are affected only due to the horizontal slot length. The corresponding effect is formulated in Equation (2). Equations (1) & (2) are derived here by extensively studying the variation in the surface currents against the half U-slot dimensions.

$$L_{e10} = L + 2h + 2L_{sv}\left(L_{sv}/1.5W\right)\cos(\pi x1/L) + 0.116\left(2L_{sh}\right)\left(L_{sh}/L\right) \tag{1}$$

$$W_{e01} = W + 2h + w_1/4 + 1/50\left(2L_{sh}\right)\left(L_{sh}/L\right)\cos(\pi y1/W) + w_2/4 \tag{2}$$

At TM_{11} mode, current variations take place along the length and width, and therefore, the resonant length formulation at the same is the combination of TM_{10} and TM_{01} mode formulations. Thus, resonant length equation at TM_{11} mode is derived by adding together the effects of half U-slot dimensions on
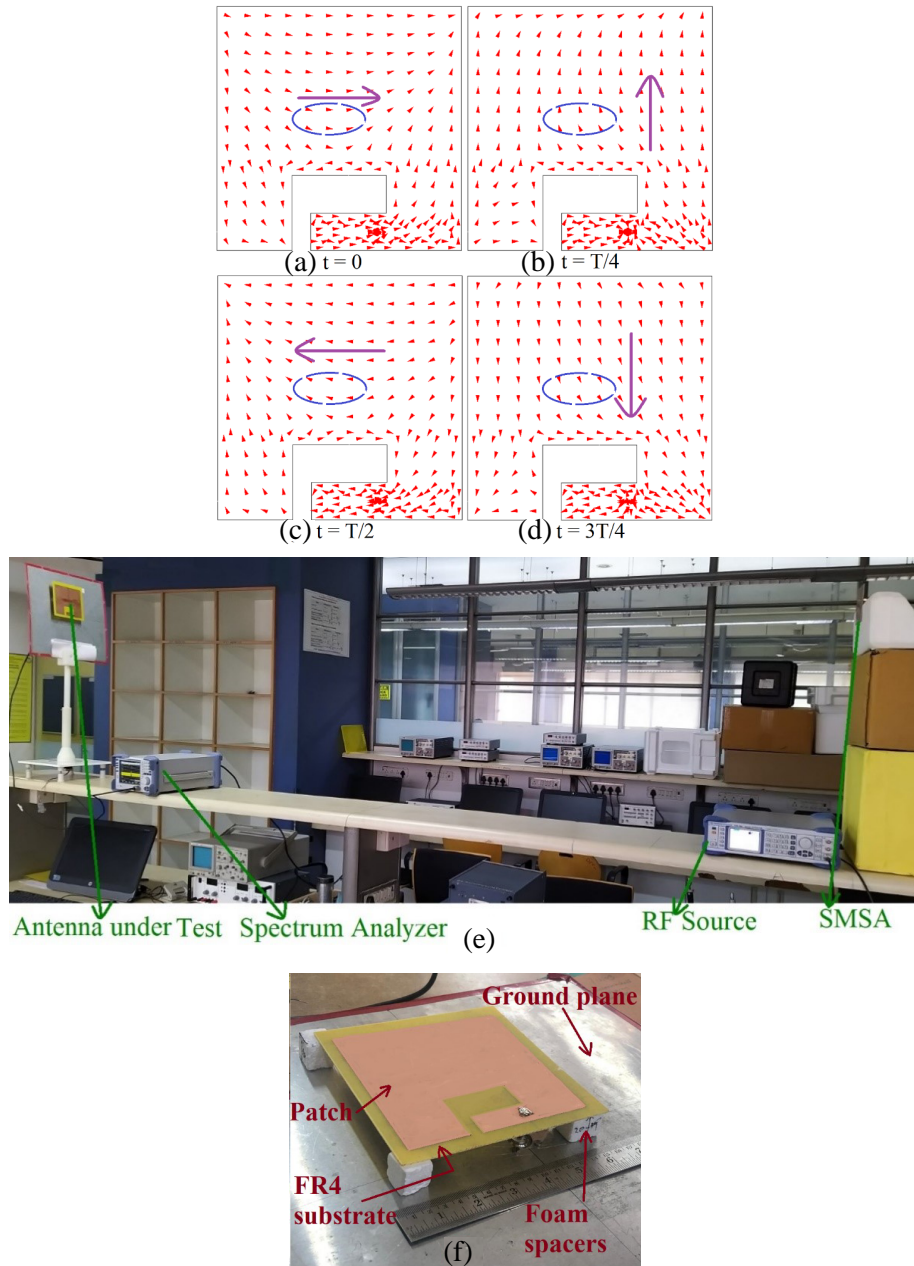
Figure 5. (a)–(d) Time varying surface current distribution at center frequency of AR bandwidth, (e) measurement setup and (f) fabricated prototype for dual band half U-slot cut SMSA.

TM_{10} and TM_{01} modes as given in Equations (1) & (2). The frequency and % error at each mode are calculated by using Equations (3) and (4), respectively. Against the total half U-slot length variation $(L_{sv} + L_{sh})$, they are plotted in Figs. 6(a)–(c). Over the complete range, a close agreement between the simulated and calculated frequencies with % error less than 5% is obtained.

$$f_{mn} = \frac{c}{2\sqrt{\epsilon_{eff}}}\sqrt{\left(\frac{m}{L_e}\right)^2 + \left(\frac{n}{W_e}\right)^2} \tag{3}$$

$$\% \, error = \left|\frac{f_{simu} - f_{calc}}{f_{simu}}\right| \times 100 \tag{4}$$
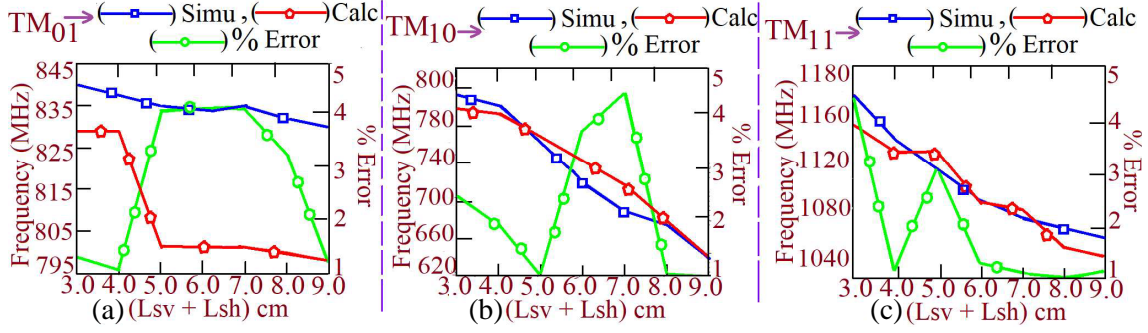
Figure 6. Frequency and % error plots at (a) TM_{01}, (b) TM_{10} and, (c) TM_{11} modes against varying total half U-slot length for the dual band half U-slot cut SMSA.

4. DESIGN METHODOLOGY FOR DUAL BAND HALF U-SLOT CUT SQUARE MSA

Using the above formulation, the redesigning procedure is explained here with reference to the center frequency (f_{CP}) of the CP response, in the second band. As noted from the above design, the simulated value of the center frequency of the CP band (f_{CP}) is 1179 MHz. Also, as observed from the parametric study, the TM_{01} mode frequency remains constant against the total half U-slot length variation. Therefore, the frequency ratio as mentioned in Equation (5) can be used to calculate the TM_{01} mode frequency of SMSA for the given f_{CP}, which will assist in the calculation of SMSA dimensions. In the proposed dual band half U-slot cut SMSA, an air suspended substrate is used, hence the calculation of the effective dielectric constant (ε_{re}) is needed. However, this requires prior knowledge of the air gap 'h_a', which is unknown to start with. Therefore, as selected in the original design, the total substrate thickness of $0.06\lambda_g$ is considered in the redesign configuration. For this thickness, an initial value of 1.06 is considered for 'ε_{re}'. This value is based upon the value of 'ε_{re}' as calculated in the above optimum design. Thus for the given 'f_{CP}' and 'ε_{re}', the TM_{01} mode frequency and total substrate thickness 'h_t' ($h_t = h_a + h$) are calculated by using Equations (5) & (6).

$$f_{01} = {f_{CP}}/{1.4} \tag{5}$$

$$h_t = 0.065 \left({30}/{f_{01}\sqrt{\varepsilon_{re}}}\right) \tag{6}$$

$$\varepsilon_{re} = {\varepsilon_r (h + h_a)}/{\varepsilon_r h_a + h} \tag{7}$$

$$L = = \left({30}/{2f_{01}\sqrt{\varepsilon_{re}}}\right) - \left({h_t}/{\sqrt{\varepsilon_{re}}}\right) \tag{8}$$

For this total substrate thickness, a practically realizable value of 'h_a' is selected. For this value of 'h_a', by using Equations (7) & (6), 'ε_{re}' and 'h_t' are recalculated. Here, 'ε_r' is the substrate dielectric constant. In the present study, a low cost FR4 substrate is chosen, which gives $\varepsilon_r = 4.3$. For this new value of 'h_t', again a practically realizable value of 'h_a' is chosen. This iterative process is carried out once since an initial assumption for 'ε_{re}' is considered. It was observed in the iterative step that the practical value of 'h_a' changes marginally. Hence, the former calculated value of 'h_a' is retained in the further design. The SMSA length 'L' for the TM_{01} mode frequency as obtained from Eq. (5) is calculated using Equation (8). Since the square patch is selected, $L = W$. With reference to the above optimum design as the reference, various patch parameters are expressed in terms of SMSA length 'L' or width 'W' as $w_1 = 0.2W$, $W_2 = 0.083L$, $x_1 = 0.166L$, $y_1 = 0.166W$, $(x_f, y_f) = (0.133L, 0.083W)$. The vertical and horizontal half U-slot lengths modify the TM_{10}, TM_{01}, and TM_{11} resonant mode frequencies to realize the dual band response. In the optimum design, observed frequency ratios are $f_{11}/f_{01} = 1.37$, $f_{01}/f_{10} = 1.379$, $f_{11}/f_{10} = 1.89$, with aspect ratios as $L_{sv1} + L_{sh1}/w_1 = 3.75$ and $L_{sv1} + L_{sh1}/w_2 = 9$. Using Equations (1)–(6), the modified f_{10}, f_{01}, and f_{11} mode frequencies against the total slot length variation are calculated. The value of total slot length, i.e., $L_{sh} + L_{sv}$, is noted which yields the above frequency and aspect ratio values. Further, the individual half U-slot length is

Table 1. Antenna parameters for the re-designed half U-slot cut SMSA at 1800 MHz.

Dimensions	Parametric Formulations	Parameter Value
$(h + h_a)$	$0.06\lambda_g$	$(1.2 + 0.16)$ cm
L, W	L_p	9.9 cm
w_1	$0.2W$	1.9 cm
w_2	$0.083L$	0.8 cm
x_1, y_1	$0.166L, 0.166W$	1.9 cm, 1.9 cm
(x_f, y_f)	$(0.133L, 0.083W)$	$(1.3, 0.8)$ cm
	Simulated	**Measured**
S_{11} bandwidth, band 1	82 MHz (6.2%)	81 MHz (6.0%)
Peak Gain, band 1	7.3 dBi	7.1 dB
S_{11} bandiwdth, band 2	330 MHz (19%)	300 (17%)
Peak Gain, band 2	7.7 dBi	7.5 dBi
f_{CP}	1772 MHz	1727 MHz
AR bandwidth	88 MHz (4.96%)	85 MHz (4.92%)

calculated by using the relation $L_{sh} = 1.25L_{sv}$. Using these guidelines, the half U-slot cut dual band SMSA is designed for 'f_{CP}' = 1800 MHz. The frequency ratio plots for the redesigned half U-slot cut SMSA are shown in Figs. 7(a)–(c). Various antenna parameters for the redesigned antenna calculated using the above procedure are given in Table 1. The redesigned antenna is simulated, and its response is experimentally verified. The results for the same are given in Fig. 7(d).

A similar response to that obtained in the original design is observed. The simulated center frequency of the CP response in the second band is 1772 MHz, which is close to the desired frequency value chosen in the initial calculation 1800 MHz. Further as observed above in Figs. 3(b) and 4(a), the center frequency of the first band lies near the TM_{01} mode frequency of SMSA. In the redesigned antenna also, TM_{01} mode frequency is 1285 MHz (as per Equation (5)), near which the first band lies. Thus, the proposed design methodology based upon the resonant length formulation is useful in realizing dual band response with first of the band lying near the TM_{01} mode frequency of SMSA, with CP characteristics around the desired frequency. The variations in the experimental results against the simulated ones are observed in the initial and redesign configurations. These are attributed to the errors in experimental setup like maintaining the exact air gap for the suspended dielectric substrate.

In the proposed configuration, for the given half U-slot orientation and coaxial feed position, the antenna yields RHCP response. The LHCP response can also be obtained in the proposed design. For this the orientation of half U-slot needs to be reversed, as shown in Figs. 8(a) and (b). The results for this LHCP antenna are similar to that of the RHCP design, except the sense of CP rotation in the second band. In the paper, to explain the antenna functioning, a resonant mode based study is presented. Another approach of analyzing the antenna response is based on the equivalent circuit model. In this the effects of modifications in the patch are added in the form of circuit elements like inductor or capacitor. The equivalent circuit for the proposed antenna is shown in Fig. 8(c).

The half U-slot lengthens the surface current length at each of the patch modes and reduces their frequencies. In the proposed design, TM_{10}, TM_{01}, and TM_{11} modes contribute to the dual band response. In the equivalent circuit, the modes (TM_{mn}) are represented by their respective parallel resonant circuit (R_{mn}, L_{mn}, C_{mn}). The reduction in the respective mode frequency against the half U-slot dimensions is different. Therefore, the reduction in each frequency is represented by additional inductor (L_{smn}), which is in series with the respective mode inductor without the half U-slot. This additional inductor reduces the respective frequency. Further, the reduction in TM_{10} mode frequency is maximum whereas that in TM_{01} mode is the lowest. Therefore, in between the three additional incremental inductors, a relation $L_{s10} > L_{s11} > L_{s01}$ exists. The parallel combination of resistance 'R' and capacitance 'C' represents the radiating and stored energy from the antenna, respectively whereas
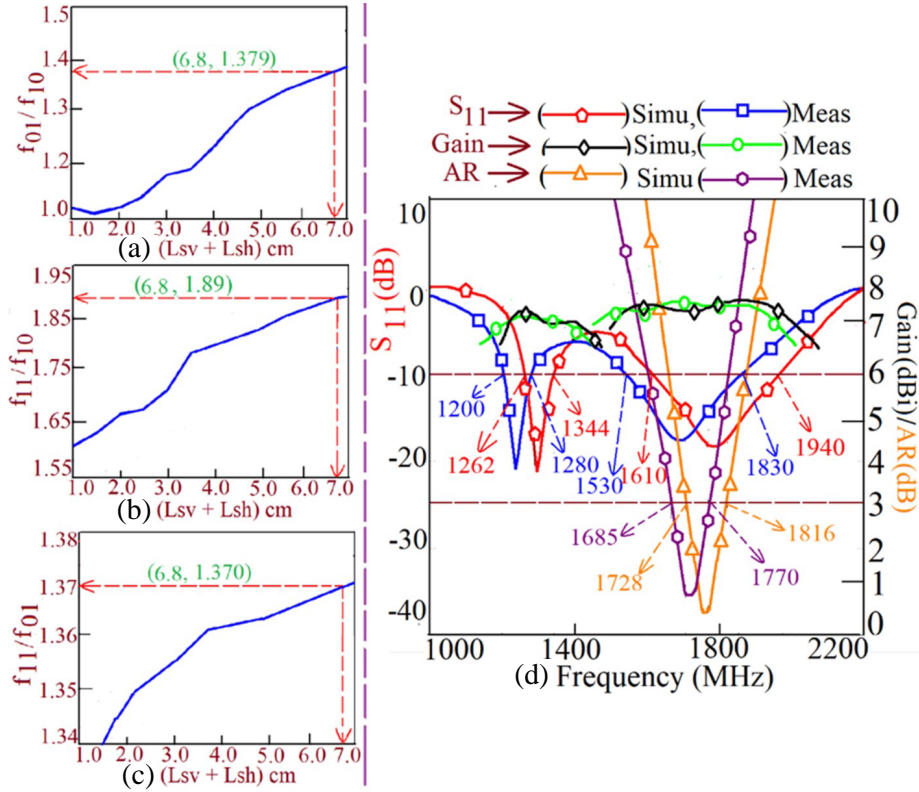
Figure 7. (a)–(c) Frequency ratio plots among TM_{10}, TM_{01}, and TM_{11} modes and (d) S_{11}, gain and AR plots for half U slot cut SMSA redesigned at $f_{cp} = 1800\,\text{MHz}$.
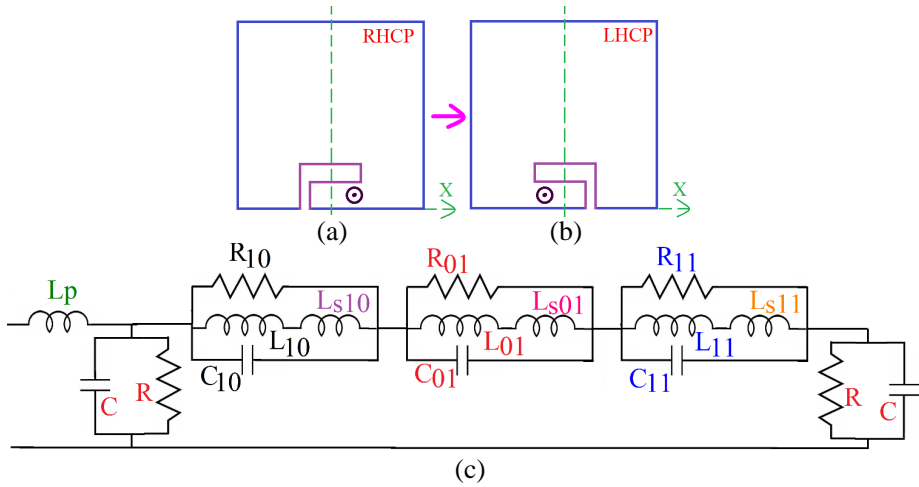
Figure 8. Dual band half U-slot cut antenna to realize (a) RHCP and (b) LHCP response, and its (c) equivalent circuit model.

the inductor 'L_p' represents the probe inductance.

Further to highlight the novelty in the proposed configuration against the reported designs, a detailed comparison is presented in Table 2. For the comparison purpose, the patch area and substrate thickness mentioned in Table 2 are normalized with respect to the center frequency of the first band in each design. Further, the frequency ratio column contains ratio value depending upon whether the configuration is dual band, triple band or other multi-band variations.

Table 2. Comparison of proposed half U-slot cut SMSA against the reported designs.

MSA shown in	f_c (f_1, f_2, f_3), bandwidth (MHz, %)	Frequency ratio	Tuning element	Peak Gain (dBi)	Area, Thickness $(A/\lambda_c, h/\lambda_c)$
Figs. 1(a), (b)	**770 (6.49), 1100 (17.36)**	**1.4**	**half U-Slot**	**8.0**	**$4.01\lambda_c, 0.055\lambda_c$**
Ref. [9]	2100 (1.8), 3600 (4.3)	1.71	ring slot	—	$0.5\lambda_c, 0.02\lambda_c$
Ref. [10]	1615 (9.1), 2492 (5.1)	1.54	stubs	3, 4.2	$0.378\lambda_c, 0.024\lambda_c$
Ref. [11]	1268 (4.5), 1575 (3.2)	1.24	—	7.47, 7.7	$0.43\lambda_c, 0.08\lambda_c$
Ref. [12]	1227 (2.0), 1575 (1.57)	1.28	slits, slots	2.68, 4.46	$0.26\lambda_c, 0.018\lambda_c$
Ref. [13]	1176 (2), 2332 (1.5)	1.98	slots	4.2, 6.6	$1.65\lambda_c, 0.006\lambda_c$
Ref. [14]	1995 (4), 2200 (3)	1.1	slot	—	$1.66\lambda_c, 0.01\lambda_c$
Ref. [15]	1176 (2.5), 1227 (2.2), 1575 (1.1), 2300 (2.7)	1.04, 1.33, 1.95	slots, slit	> 2.2	$2.6\lambda_c, 0.02\lambda_c$
Ref. [16]	1176 (5.16), 1227 (3.68), 1575 (1.45)	1.04, 1.33	slots	4.65	$3.2\lambda_c, 0.024\lambda_c$
Ref. [17]	2445 (5), 3355 (2), 4360 (9)	1.37, 1.78	stubs, slots	7.5, 8.7, 87	$0.86\lambda_c, 0.04\lambda_c$
Ref. [18]	2400 (3.6), 5800 (4.3)	2.33	PIN diode	4.2, 6	$1.64\lambda_c, 0.05\lambda_c$

An empirical formulation provided for the dual band CP MSA in [9] is very complex as the resonant length formulation based on patch parameters is not explained. Further, higher frequency ratio between the two bands does not allow the suitable frequency or polarization agility. In spite of using a thicker substrate, the realized impedance bandwidth is less for the dual band CP MSAs as reported in [10–12]. For altering the sense of polarization, a design using multiple slots on the main patch is reported for the dual polarized multi-band response [13]. However, due to the multiple patches, the design has a higher degree of fabrication complexity. The dual polarized or circularly polarized multi-band configurations as reported in [14–17] lack in providing an in-depth explanation for the effects of slots, stubs, or shorting posts on the patch resonant modes and their impedances, in achieving the said response. The reconfigurable active devices along with their biasing circuits increase the integration and fabrication complexity for the dual polarized multi-band configurations as reported in [18–20]. The dual band E-shape MSA as reported in [25] offers higher frequency ratio than the proposed design. The CP designs using U-slot variations yields measured impedance and AR bandwidth of 11.2% and 3.9%, respectively, with a peak gain of 9 dBi, on a substrate of thickness $0.08\lambda_g$ [28]. Further, on a substrate of thickness $0.09\lambda_g$, U-slot cut CP SMSA yields impedance and AR bandwidth of 9% and 4%, respectively with peak gain of 8 dBi [30]. Against these, the proposed design offers comparable values of AR bandwidth and gain but a higher impedance bandwidth using a half U-slot. The U-slot cut SMSA reported in [29] does offer wide AR bandwidth, but it employs a dual feed and power divider network. The U-slot cut CP design reported in [31] yields wide AR bandwidth, but it requires a substrate thickness of $0.2\lambda_g$. The U-slot cut SMSA for CP response as reported in [32] yields 3.2% of AR bandwidth and gain of 4.5 dBi, on a substrate of thickness $0.05\lambda_g$. In comparison, the proposed design offers higher gain. The E-shape and modified E-shape (ψ-shape) designs reported in [33, 34] offer AR bandwidth greater than 5% in single or dual bands, but they require larger patch size. A compact design of E-shape MSA using a single rectangular slot is reported in [35]. It yields 5.3% of AR bandwidth with substrate thickness of $0.09\lambda_g$. In comparison, the proposed design requires lower substrate thickness and offers comparable value of the antenna gain. Further, in none of the reported resonant slot cut antennas for the CP response, a dual band response is achieved. Against those, in the proposed design, a dual band response is obtained with more than 5% impedance bandwidth in each band, which helps in frequency agile applications. Further, the reported work does not provide any design methodology to realize CP response around the given frequency band, which is presented here. The characteristics

mode based analysis is reported for E-shape and U-slot cut CP antennas [36]. However, this approach does not provide any design methodology, which is presented in this work by studying the respective resonance curve plots and modal surface current distributions against the varying slot dimensions.

Thus to summarize, against the reported designs, the proposed configuration employs a simple coaxial feed SMSA geometry embedded with an offset half U-slot, for the realization of the dual band response with a circular polarization in the second band, while offering smaller frequency ratio (1.4) between the two operating bands. The proposed configuration is fabricated on an air suspended low cost FR4 substrate, which reduces the overall cost of the antenna. Further as air suspended substrate is used ($h_t \sim 0.06\lambda_g$), it realizes appreciable value of the gain and bandwidth. More importantly, an in-depth parametric analysis is presented to explain the effects of slot on various antenna modes. Using this a design methodology is presented that lacks in most of the reported papers. Thus, in contrast with the reported papers, this paper presents a simple coaxially fed slot cut SMSA for the dual band circularly polarized response. The design fabricated on an air suspended FR4 substrate yields measured impedance bandwidths of 6.49% and 17.36%, with a broadside gain > 7.0 dBi, in the two bands. In equivalence to the area of SMSA without the slot working in the first band frequency, the proposed design offers 8% reduction in the patch area. Using a half U-slot, more than 3% AR bandwidth is achieved, which is comparable with that obtained in the reported U-slot cut CP MSAs, but with a reduced patch width. These are all the new technical contributions in the proposed work against the reported multi-band and resonant slot cut CP MSAs. With reference to the operating frequency band realized in the proposed design, half U-slot cut SMSA finds applications in GSM750 and GPS L5 band systems.

5. CONCLUSIONS

A design of half U-slot cut SMSA is presented for the dual band and circularly polarized response. An offset half U-slot using unequal slot width is employed that tunes the inter-spacing between the TM_{10}, TM_{01}, and TM_{11} resonant modes and modifies the surface current distributions at them, to yield dual band response with circular polarization in the second band. The optimized configuration yields impedance bandwidths of 6.49% and 17.36% in the two bands with a peak broadside gain of > 7.0 dBi. In the second band, more than 3% of the AR bandwidth is achieved using a compact half U-slot. The optimized configuration entirely covers the GSM 750 and GPS L5 bands, offering 8% reduction in the patch area against the similar square patch in the lower frequency range. A design methodology using resonant length formulation is presented that helps in realizing a similar configuration in the given specific frequency band as per the desired application.

REFERENCES

1. Kumar, G. and K. P. Ray, *Broadband Microstrip Antennas*, 1st Edition, Artech House, USA, 2003.
2. Garg, R., P. Bhartia, and I. Bahl, *Microstrip Antenna Design Handbook*, London Artech House, 2001.
3. Wong, K. L., *Compact and Broadband Microstrip Antennas*, 1st Edition, John Wiley & Sons, Inc., New York, USA, 2002.
4. Balanis, C. A., *Antenna Theory & Design*, 3rd Edition, John Wiley & Sons Inc. Publication, 2005.
5. Heidari, A. A., M. Heyrani, and M. Nakhkash, "A dual-band circularly polarized stub loaded microstrip patch antenna for GPS applications," *Progress In Electromagnetics Research*, Vol. 92, 195–208, 2009.
6. Khidre, A., F. Yang, and A. Z. Elsherbeni, "A patch antenna with a varactor-loaded slot for reconfigurable dual-Band operation," *IEEE Transactions on Antennas and Propagation*, Vol. 63, No. 2, 755–760, 2015.
7. Cao, W., Q. Wang, B. Zhang, and W. Hong, "Capacitive probe-fed compact dual-band dual-mode dual-polarization microstrip antenna with broadened bandwidth," *IET Microwave Antennas & Propagation*, Vol. 11, No. 7, 1003–1008, 2017.

8. Liu, S., W. Wu, and D. G. Fang, "Single-feed dual-layer dual-band e-shaped and u-slot patch antenna for wireless communication application," *IEEE Antennas and Wireless Propagation Letters*, Vol. 15, 468–471, 2015.

9. Liang, Z.-X., D. C. Yang, X. C. Wei, and E. P. Li, "Dual-band dual circularly polarized microstrip antenna with two eccentric rings and an arc-shaped conducting strip," *IEEE Antennas and Wireless Propagation Letters*, Vol. 15, 834–83, 2016.

10. Yang, H., Y. Fan, and X. Liu, "A compact dual-band stacked patch antenna with dual-circular polarizations for BeiDou navigation satellite systems," *IEEE Antennas and Wireless Propagation Letters*, Vol. 18, No. 7, 1472–1476, 2019.

11. Li, Y., B. Tian, J. Xue, and G. Ge, "Compact dual-band circularly polarized antenna design for navigation terminals," *IEEE Antennas and Wireless Propagation Letters.* Vol. 1, No. 15, 802–805, 2015.

12. Agarwal, K., Y. X. Guo, Nasimuddin, and A. Alphones, "Dual-band circularly polarized stacked microstrip antenna over RIS for GPS applications," *2013 IEEE International Wireless Symposium (IWS)*, 1–4, 2013.

13. Surya, D. S., D. Choudhary, A. Srivastava, and M. Manish Kumar, "Design of single-fed dual-polarized dual-band slotted patch antenna for GPS and SDARS applications," *Microwave and Optical Technology Letters*, Vol. 63, 353–360, 2020.

14. Liao, W. and Q. X. Chu, "Dual-band circularly polarized microstrip antenna with small frequency ratio," *Progress In Electromagnetics Research Letters*, Vol. 15, 145–152, 2010.

15. Falade, O. P., M. Ur-Rehman, X. Yang, G. A. Safdar, C. G. Parini, and X. Chen, "Design of a compact multiband circularly polarized antenna for global navigation satellite systems and 5G/B5G applications," *International Journal of RF and Microwave Computer-Aided Engineering*, Vol. 30, No. 6, 1–13, 2020.

16. Nasimuddin, X. Qing, and Z. N. Chen, "A compact circularly polarized slotted patch antenna for GNSS Applications," *IEEE Transactions on Antennas and Propagation*, Vol. 62, No. 12, 6506–6509, 2014.

17. Tan, Q. and F. C. Chen, "Triband circularly polarized antenna using a single patch," *IEEE Antennas and Wireless Propagation Letters*, Vol. 19, No. 12, 2013–2017, 2020.

18. Qin, P., Y. J. Guo, and C. A. Ding, "Dual-band polarization reconfigurable antenna for WLAN Systems," *IEEE Transactions on Antennas and Propagation*, Vol. 61, No. 11, 5706–5713, 2013.

19. Kim, B., B. Pan, S. Nikolaou, Y. Kim, J. Papapolymerou, and M. M. Tentzeris, "A novel single-feed circular microstrip antenna with reconfigurable polarization capability," *IEEE Transactions on Antennas and Propagation*, Vol. 56, No. 3, 630–638, 2008.

20. Fakharian, M. M., P. Rezaei, and A. A. Orouji, "Reconfigurable multiband extended U-Slot antenna with switchable polarization for wireless applications," *IEEE Antennas and Propagation Magazine*, Vol. 57, No. 2, 1–9, 2015.

21. Deshmukh, A. A. and G. Kumar, "Compact broadband U-slot-loaded rectangular microstrip antennas," *Microwave and Optical Technology Letters*, Vol. 46, No. 6, 556–559, 2005.

22. CST Microwave Studio, Version 2019.

23. Deshmukh, A. A. and K. P. Ray, "Formulation of resonance frequency for dual band slotted rectangular microstrip antennas," *IEEE Magazine on Antennas and Propagation*, Vol. 54, No. 4, 78–97, 2012.

24. Deshmukh, A. A. and K. P. Ray, "Analysis and design of broadband U-slot cut rectangular microstrip antennas," *Sadhana*, Vol. 42, No. 10, 1671–1684, Academy Proceedings in Engineering Science, Springer Publication, 2017.

25. Ambekar, A. G. and A. A. Deshmukh, "E-shape microstrip antenna for dual frequency WLAN application," *Progress In Electromagnetic Research C*, Vol. 104, 13–24, 2020.

26. Lee, K. F., S. L. Yang Steven, A. A. Kishk, and K. M. Luk, "The versatile U-slot patch antenna," *IEEE Antennas and Propagation Magazine*, Vol. 52, No. 1, 71–88, 2010.

27. Deshmukh, A. A. and K. P. Ray, "Analysis of broadband variations of U-slot cut rectangular microstrip antennas," *IEEE Magazine on Antennas and Propagation*, Vol. 57, No. 2, 181–193, 2015.

28. Lee, K. F., K. M. Luk, W. C. Mok, and P. Nayeri, "Single probe-fed circularly polarized patch antennas with U-slots," *Microwave and Optical Technology Letters*, Vol. 53, No. 6, 1245–1253, 2011.

29. He, M., X. Ye, P. Zhou, G. Zhao, C. Zhang, and H. Sun, "A small-size dual-feed broadband circularly polarized U-slot patch antenna," *IEEE Antennas and Wireless Propagation Letters*, Vol. 14, 898–901, 2015.

30. Tong, K.-F. and T.-P. Wong, "Circularly polarized U-slot antenna," *IEEE Transactions on Antennas and Propagation*, Vol. 55, No. 8, 2382–2385, 2007.

31. Yang, S., K. F. Lee, A. Kishk, and K.-M. Luk, "Design and study of wideband single feed circularly polarized microstrip antennas," *Progress In Electromagnetics Research*, Vol. 80, 45–61, 2008.

32. Lam, K. Y., K.-M. Luk, K. F. Lee, H. Wong, and K. B. Ng, "Small circularly polarized U-slot wideband patch antenna," *IEEE Antennas and Wireless Propagation Letters*, Vol. 10, 87–90, 2011.

33. Khidre, A., K. F. Lee, F. Yang, and A. Eisherbeni, "Wideband circularly polarized E-shaped patch antenna for wireless applications," *IEEE Antennas and Propagation Magazine*, Vol. 52, No. 5, 219–228, 2010.

34. Deshmukh, A. A. and A. A. Odhekar, "Dual band circularly polarized modified ψ-shape microstrip antenna," *Progress In Electromagnetics Research C*, Vol. 115, 161–174, 2021.

35. Kovitz, J. M., H. Rajagopalan, and Y. Rahmat-Samii, "Circularly polarised half E-shaped patch antenna: A compact and fabrication-friendly design," *IET Microwaves, Antennas & Propagation*, Vol. 10, No. 9, 932–938, 2016.

36. Chen, Y. and C.-F. Wang, "Characteristic mode based improvement of circularly polarized U-slot and E-shaped patch antennas," *IEEE Antennas and Wireless Propagation Letters*, Vol. 11, 1474–1477, 2012.